analytical chemistry

Article

pubs.acs.org/ac

DNA-Templated Silver Nanoclusters for Fluorescence Turn-on Assay of Acetylcholinesterase Activity

Yaodong Zhang,*[,†] Yanan Cai,[†] Zongli Qi,[‡] Lu Lu,[†] and Yunxia Qian[†]

[†]Key Laboratory of Applied Surface and Colloid Chemistry, Ministry of Education, Key Laboratory of Analytical Chemistry for Life Science of Shaanxi Province, School of Chemistry and Chemical Engineering, Shaanxi Normal University, Xi'an 710062, PR China

[‡]Lab Center, the Third Affiliated Hospital, Xi'an Jiaotong University, Xi'an 710049, PR China

Supporting Information

ABSTRACT: We have developed a fluorescence turn-on assay using DNA-templated silver nanoclusters (Ag NCs) (i.e., 12 polycytosine-templated silver nanoclusters, dC_{12}–Ag NCs), which is amenable to rapid, ultrasensitive assay of acetylcholinesterase (AChE). The detection mechanism is based on the concept, that is, AChE hydrolyzes the acetylthiocholine (ATCh) chloride to produce thiocholine (TCh). Subsequently, TCh sensitively and rapidly reacts with dC_{12}–Ag NCs via Ag–S bond forming and enhances the fluorescence of dC_{12}–Ag NCs. Using dC_{12}–Ag NCs, detection of TCh has a linear concentration range of 2.0 nM to 16.0 nM and a detection limit of 0.3 nM. Due to the sensitive and rapid fluorescence turn-on response of dC_{12}–Ag NCs to TCh, AChE with activity as low as 0.5×10^{-4} U/mL (signal/noise = 3) can be analyzed with a dynamic range of 0.1 to 1.25×10^{-3} U/mL. The promising application of the proposed method in AChE inhibitor screening was demonstrated. AChE concentrations were determined in human blood red cell (RBC) membranes from clinical specimens using dC_{12}–Ag NCs, and the quantitative results were validated with Ellman's method. Aside from the ease of manufacture, reduction of matrix effect, and low background noise, the continuous detection format and detection sensitivity can open up to wider applications to AChE activity assay in neurobiology, toxicology, and pharmacology, among other fields.

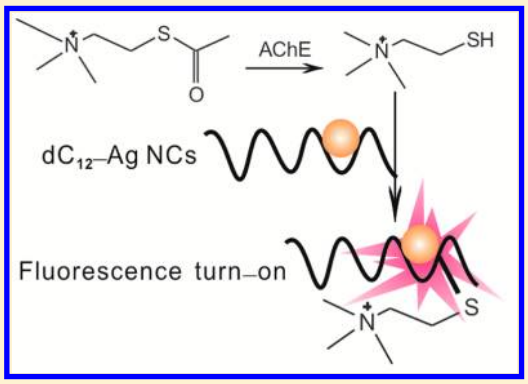

Acetylcholinesterase (AChE) terminates synaptic transmission at cholinergic synapses through rapid hydrolysis of acetylcholine (ACh) and has pivotal functions in Alzheimer's disease, inflammatory processes, and nerve-agent poisoning.[1] AChE inhibitors that penetrate the blood-brain barrier have been useful in the symptomatic treatment of Alzheimer's disease and are the principal drugs.[2] Moreover, organophosphate poisoning is frequently diagnosed through an AChE inhibition assay.[3] Therefore, a reliable sensitive assay method for AChE activity is applicable to a very wide range of fields, including pharmaceutical, healthcare, food and agricultural industries, and environmental monitoring.

A sensitive and low cost method for determining AChE activity in biological samples and for discovering new drugs is needed. Ellman's colorimetry is the technique mostly applied in the determination of cholinesterase activity. This technique is the gold standard for the evaluation of AChE activity and allows a wide scale of experiments to be performed.[4] However, this method is limited by its low sensitivity, which causes false-negative results [e.g., the molar extinction coefficient of 5-thio-2-nitrobenzoic acid (TNB) at 412 nm is 14150 $L \cdot mol^{-1} \cdot cm^{-1}$],[5] and potential matrix effects, which cause false positive-results (e.g., the massive Soret absorbance of hemoglobin interferes with the absorbance of TNB).[6] Various methods[7] have been developed over the past decades for AChE quantification, such as colorimetric,[7b] chemiluminescent,[7c] fluorescent,[7d,i] electrochemical,[7j] and interferometric.[7k] However, certain drawbacks still exist,[7l] such as long measuring time, low detection sensitivity, disturbances by the sample matrix, use of other enzymes for signal amplification and readout, insufficient specificity of substrates, and laborious sample preparation.

Fluorometric approaches employed with dye fluorophores[7d–f] or quantum dots[7g] have been reported for assays of AChE activity and screening of AChE inhibitors, which provide higher sensitivities and lower detection limits. Although dye molecules are small and nontoxic, the existing dye molecules have the disadvantages of rapid bleaching and insufficient emission intensities.[8] Although quantum dots have high fluorescence quantum yields and very strong absorption and size-tunable emissions, they present a number of issues, including large physical size and strong fluorescence intermittency on all time scales.[9] Therefore, a new, simple, sensitive, and rapid method for AChE activity assay and inhibitor screening is still highly needed.

The emerging technology of fluorescent few-atom silver nanoclusters (Ag NCs) offers an attractive compromise

Received: June 30, 2013
Accepted: August 6, 2013
Published: August 6, 2013

   dx.doi.org/10.1021/ac401966d | *Anal. Chem.* 2013, 85, 8455–8461

between the photostability and brightness of quantum dots and the compact versatility of dye fluorophores. This technology has recently received considerable attention in a wide range of chemical or biological detection and cellular imaging applications.[10] For instance, DNA−AgNCs have been applied to the transfection of HeLa cells,[10g] live cell surface labeling,[11] intracellular staining,[10j] DNA single-nucleotide mutation discrimination,[10d] specific protein detection,[12] and conjugation of chromophoric reporters and DNA ligands.[10i] Sensors for thiolated molecules, such as cysteine (Cys), glutathione (GSH), and homocysteine, which interact strongly with Ag NCs, have been also reported in literature.[13,14]

In this study, a new phenomenon, wherein the fluorescence of 12 polycytosine-templated silver nanoclusters (dC_{12}−Ag NCs) can significantly increase because of the reaction of dC_{12}−Ag NCs with thiocholine (TCh), has been observed. Furthermore, this new property was maximized for the fluorescence turn-on ultrasensitive detection of AChE activity. The fluorescence assay for AChE activity is illustrated in Scheme 1. Acetylthiocholine (ATCh) chloride underwent

Scheme 1. Principal Reactions of Fluorescence Assay for AChE Activity[a]

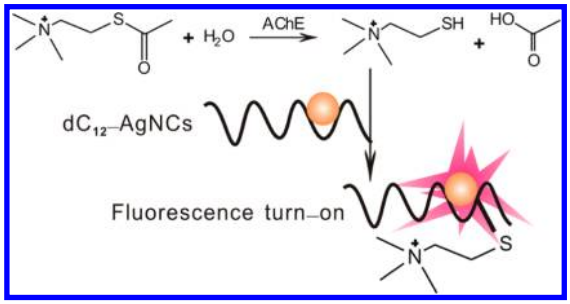

[a]AChE hydrolyzes ATCh and produces TCh, which in turn reacts with dC_{12}−Ag NCs to enhance the fluorescence of dC_{12}−Ag NCs.

catalytic hydrolysis to produce TCh upon the addition of AChE. Afterward, TCh reacted with dC_{12}−Ag NCs that led to the formation of a complex via Ag−S bonds. Accordingly, the fluorescence of dC_{12}−Ag NCs increased significantly. The hydrolysis of ATCh chloride was retarded in the presence of the corresponding inhibitor. Thus, AChE activity and inhibition can be analyzed using dC_{12}−Ag NCs. The fluorescence turn-on assay on AChE activity in human blood red cell (RBC) membranes was also demonstrated.

EXPERIMENTAL SECTION

Materials and General Methods. AChE (from *Electrophorus electricus*), ATCh chloride, ATCh iodide, 5,5′-dithiobis-(2-nitro-benzoic acid) (DTNB), tacrine, galanthamine, GSH, Cys, human serum albumin (HSA), calf intestinal alkaline phosphatase (CIAP), and lipase were purchased from Sigma-Aldrich (Peking, China) and used without further purification. Lysozyme (Lys) and all oligonucleotides used in this study were synthesized and purified by Shanghai Sangon Biotechnology Co. Ltd. (Shanghai, China), and all the oligonucleotide sequences are listed in Table S1. Silver nitrate (99.99%), sodium borohydride ($NaBH_4$ powder, 98%), and other chemicals were obtained from Alfa-Aesar (Tianjing, China) and used as received. TCh chloride was synthesized and characterized according to the method described in a previous study.[7d] All solutions were prepared using Millipore Milli-Q water (18.2 MΩ cm). UV−visible spectra were obtained using a UV-2450 spectrophotometer (Shimadzu, Japan). Fluorescence spectra were obtained using a Cary Eclipse fluorescence spectrophotometer (Varian, U.S.A.) at room temperature. Automatic hemocytometer (SYSMEX XE-2100, Japan) was used for red blood cell (RBC) counting. Circular Dichroism (CD) spectra were measured on a Chirascan CD Spectrometer (Applied Photophysics, England). X-ray photoelectron spectroscopy (XPS) measurements were carried out on an AXIS ULTRA photoelectron spectrometer (Kratos Analytical, England).

Preparation of DNA−Ag NCs. A complete list of DNA strands used in this study can be found in Table S1 of the Supporting Information. DNA−Ag NCs were synthesized according to the modifications described in the literature.[10a] The high affinity of Ag^+ for DNA bases enabled the creation of DNA−Ag NCs without the formation of large nanoparticles.[10h] Briefly, a DNA strand was first dissolved in 5.0 mM pH 7.0 sodium phosphate buffer. Ag NCs were formed by adding $AgNO_3$ to the DNA solution, and then followed by reduction with $NaBH_4$. The final concentrations were 10 μM DNA, 60 μM $AgNO_3$, and 60 μM $NaBH_4$ in 5.0 mM pH 7.0 sodium phosphate buffer. The aqueous solution of $NaBH_4$ was freshly prepared by dissolving $NaBH_4$ powder in water and adding the required volume to the DNA/Ag^+ mixture within 30 s, followed by vigorous shaking for 1 min. The reaction was kept in the dark at room temperature for 2 h and 4 °C overnight. The DNA-Ag NCs was diluted with 5.0 mM pH 7.0 sodium phosphate buffer to reach the appropriate concentration for further use.

The dC_{12}−Ag NCs for AChE determination. The activity of commercial AChE was first determined using the Ellman method for validation (Supporting Information S3). AChE was diluted to a low amount of 5.0 mM pH 7.0 sodium phosphate buffer. The diluted AChE was then added to a solution of dC_{12}−Ag NCs (2.0 μM) and ATCh chloride (8.0 μM) in phosphate buffer (5.0 mM, pH 7.0). The resulting solution was incubated at 25 °C for a certain period, and its fluorescence spectrum was measured, respectively. The fluorescence intensity of dC_{12}−Ag NCs at 635 nm was plotted as a function of the incubation time of AChE (up to 5 min). The change in fluorescence intensity per unit time per cuvette, which represents the activity of AChE, was calculated from the slope of each straight line. A blank cuvette containing substrates without AChE was prepared as the control for the nonspecific hydrolysis of the substrates. The limit of detection (LOD) of this method was obtained from the equation: LOD = $3S_0/S$, wherein S_0 is the standard deviation of the background and S is the sensitivity.

Noncovalent Inhibition of AChE. Inhibitors were preincubated at varying concentrations (0 nM to 20.0 nM for tacrine and 0 nM to 40.0 nM for galanthamine) with AChE (0.75×10^{-3} U/mL) in phosphate buffer (5.0 mM, pH 7.0) at 25 °C for 15 min. After which, dC_{12}−Ag NCs (2.0 μM) and ATCh chloride (8.0 μM) were added. The fluorescence intensities were recorded at 635 nm for a certain period, respectively. The inhibition efficiency was determined after the measurement of AChE activity in the presence and absence of the inhibitors, based on the formula, $[A_0 - A_i/A_0] \times 100$, wherein A_0 is the initial activity (the change in fluorescence intensity per unit time (i.e., slope), without inhibitor incubation) and A_i is the remaining activity (the change in fluorescence intensity per unit time, with inhibitor incubation).

dx.doi.org/10.1021/ac401966d | Anal. Chem. 2013, 85, 8455−8461

The inhibition ability of an inhibitor was described by the IC_{50} value, which refers to the inhibitor concentration required for 50% inhibition of enzyme activity. The IC_{50} value was obtained from the plot of inhibition efficiency versus inhibitor concentration.

Preparation of RBC Membranes and Determination of Its AChE Activity. Fresh blood was drawn from the antecubital vein of healthy volunteers from a local hospital using sodium citrate as an anticoagulant. Fresh blood was centrifuged at 1000 g for 10 min. RBCs were separated from plasma and buffy coat and then washed three times with isotonic phosphate buffer [10 mM NaH_2PO_4/Na_2HPO_4, 5 mM KCl, and 140 mM NaCl (pH 7.4)]. RBC membranes were prepared by hypotonic hemolysis according to the method described by Hammond et al.[15] with minor modifications. Briefly, RBCs were lysed in ice-cold water, vortexed, and then incubated for 10 min at 4 °C. The cell membranes were isolated by 8 to 10 cycles of repeated centrifugation (15,000 g, 20 min) and then rinsed with sodium phosphate buffer (10 mM, pH 7.4) until slightly pink. The final white pelleted cell membranes were resuspended in the same buffer and stored at −40 °C. The AChE activity of the RBC membranes was initially determined using Ellman's method for validation (Supporting Information S3). AChE activity was then determined using dC_{12}−Ag NCs by the aforementioned procedure after the RBC membranes were diluted with 5.0 mM pH 7.0 sodium phosphate buffer. For both AChE activities, the values were calculated per RBC. An automatic hemocytometer was used for RBC counting.

RESULTS AND DISCUSSION

Interaction of DNA-Ag NCs with TCh and Possible Mechanism. The fluorescent Ag nanoclusters were successfully prepared with dC_{12} strand (Table S1, Supporting Information) as the synthesis template. The UV−vis absorption spectrum of DNA−Ag NCs (Figure 1A, curve a) showed two peaks at 442 and 547 nm. Electronic transitions for small silver clusters, in particular Ag_2 and Ag_3, are expected in this spectral region.[10a,16,17] However, no change in the absorbances or peak positions was observed when the solutions were centrifuged, indicating that the spectra cannot be attributed to nanoparticles. Upon excitation at 570 nm, the dC_{12}−Ag NCs showed a maximum emission at 635 nm (Figure 1A, curve c and curve d). However, no fluorescence emission occurred upon excitation at 442 nm. When TCh was added to the dC_{12}−Ag NCs solutions, the fluorescence of dC_{12}−Ag NCs greatly increased as a function of TCh concentration (Figure 1B). For instance, the fluorescence intensity at 635 nm for the aqueous solution of dC_{12}−Ag NCs (2.0 μM) was enhanced by about ~3.5 times when the concentration of TCh reached 20.0 nM. Moreover, the fluorescence intensity of the dC_{12}−Ag NCs solution increased almost linearly with the concentration of TCh at the range of 2.0 nM to 16.0 nM, with a very low detection limit of 0.3 nM, as displayed at the inset of Figure 1. The enhancement of fluorescence reached a constant value in less than 1 min by monitoring the response time of dC_{12}−Ag NCs at different amounts of TCh, revealing the fast response of dC_{12}−Ag NCs to TCh (Supporting Information, Figure S1).

A series of DNA templates with different lengths and base compositions were employed for Ag NCs synthesis to study the template-dependent responses of DNA-Ag NCs to TCh (Supporting Information, Table S1). The results showed that different fluorescent response patterns (reduction or enhancement) toward TCh can be observed using different DNA templates (Figure 1B and Figure S2, Supporting Information). One possible mechanism is the change in microenvironment provided by the different DNA templates.[10i] This result is supported by CD spectra (Figure S3, Supporting Information). As shown in the CD spectra, Ag^+ preferentially bonded with the bases and significantly affected DNA conformation, as evidenced by the development of two strong peaks with negative ellipticity at 215 and 265 nm and by the decreased ellipticity of the peak at 290 nm. These results are consistent with prior studies.[10a,18] All CD spectra changed upon the reduction of Ag^+ with $NaBH_4$. However, the differences in CD spectra among the DNA−Ag NCs indicate that the Ag NCs induce more structural changes in DNA than Ag^+ (Figure S3, Supporting Information and Figure 2). The different structures of DNA template possibly caused the different DNA−Ag NCs to have different fluorescence responses to TCh (Figure 2A). By contrast, the addition of TCh yielded no structural changes in the same DNA−Ag NCs (Figure S3, Supporting Information). These results demonstrate that the enhancement phenomenon observed in the response of dC_{12}−Ag NCs to TCh is not caused by structural changes. The fluorescence enhancement can be attributed to ligand-to-metal charge

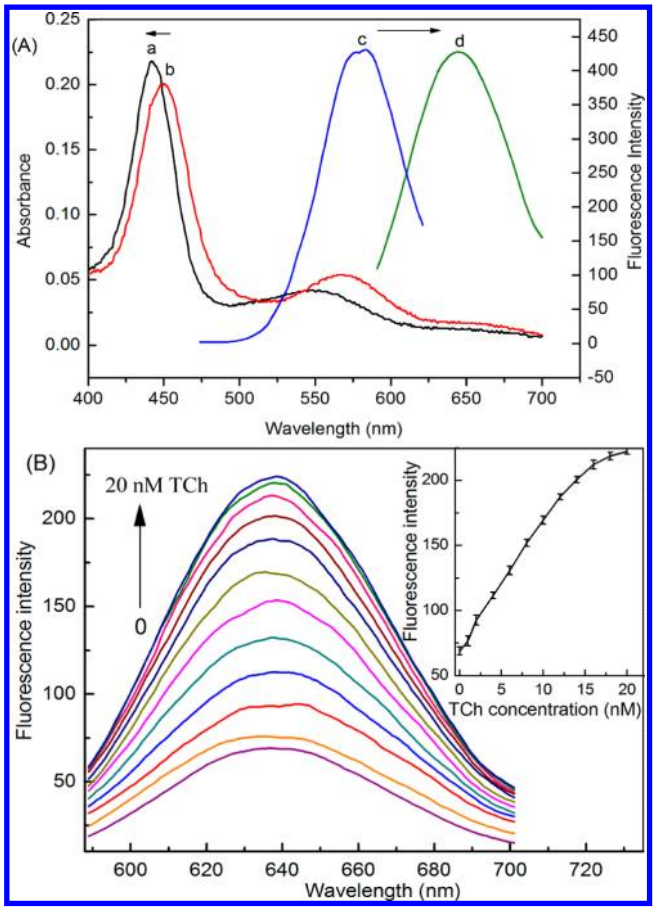

Figure 1. (A) Absorption spectra of 10 μM of dC_{12}−Ag NCs before (curve a) and after (curve b) adding 3 μM of TCh and excitation (curve c) and emission (curve d) fluorescence spectra of the obtained 10 μM dC_{12}−Ag NCs. (B) Fluorescence response of dC_{12}−Ag NCs to TCh. dC_{12}−Ag NCs (2.0 μM) in the presence of different concentrations of TCh (0.0, 1.0, 2.0, 4.0, 6.0, 8.0, 10.0, 12.0, 14.0, 16.0, 18.0, and 20.0 nM). The inset shows the plot of fluorescence intensity of dC_{12}−Ag NCs at 635 nm versus the TCh concentration.

dx.doi.org/10.1021/ac401966d | Anal. Chem. 2013, 85, 8455−8461

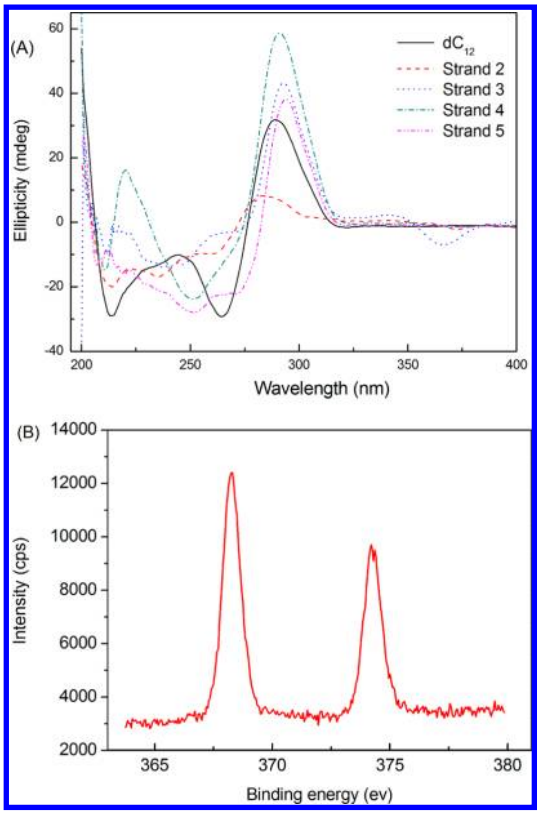

Figure 2. (A) Circular dichroism of different DNA-templated Ag NCs (10.0 μM) with TCh (2.0 μM); (B) XPS spectra of dC_{12}–Ag NCs (10.0 μM) with TCh (2.0 μM). The peak for Ag $3d_{5/2}$ in the DNA–Ag NCs occurs at 368.3 eV.

transfer (LMCT) or ligand-to-metal–metal charge transfer (LMMCT) from the sulfur atom in the thiolate ligands to Ag atoms and to the subsequent radiative relaxation, most likely through a metal-centered triplet state.[19−21] The formation of Ag–S bonds was demonstrated by the absorption red shift (Figure 1A, Curve b), which was due to the sulfur atom acting as an electron donor[22] and the presence of the peak for Ag $3d_{5/2}$ at 368.3 eV in the XPS spectra[23]of Ag NCs after the addition of TCh (Figure 2B). The formation of the Ag–S bonds indicates that charge transfer can occur between dC_{12}–Ag NCs and TCh. The effects of ATCh chloride on the fluorescence of dC_{12}–Ag NCs were also determined to ensure that the observed fluorescence enhancement is due to the formation of the Ag–S bond. No fluorescence changes were observed in the control experiments (Figure 3).

Other combined mechanisms possibly drive a fast and sensitive response. Thiol can strongly bond to silver because the interaction of the sulfur atom with the sp bands stabilizes the bond to the surface at equilibrium position.[24] The binding energy values of the system are strongly dependent on the distances from the surface. The equilibrium distance to the surface of the adsorbed sulfur atom is approximately 2 Å, depending on the adsorption site.[25] In addition, the quaternary ammonium group of TCh is positively charged,[26] whereas DNA molecules are negatively charged because of existing phosphate groups. Thus, the electrostatic interactions between dC_{12} and TCh resulted in the sensitive and rapid response of dC_{12}–Ag NCs to TCh, contributing to the proximity and stabilization of TCh to the equilibrium position of the silver atom.

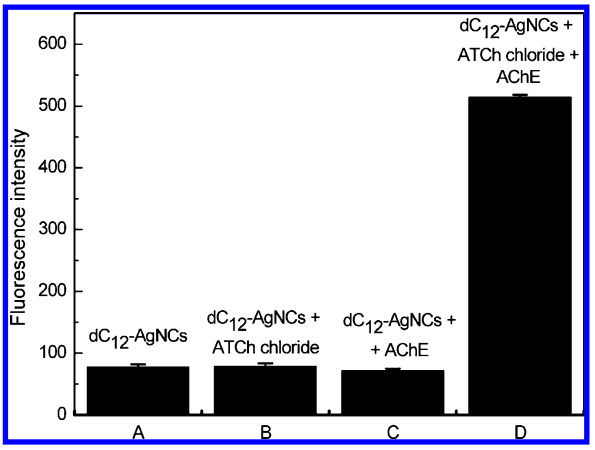

Figure 3. Variation of the fluorescence intensity at 635 nm under different conditions. (A) 2.0 μM dC_{12}–Ag NCs; (B) 2.0 μM dC_{12}–Ag NCs and 8 μM ATCh chloride; (C) dC_{12}–Ag NCs and 0.002 U/mL AChE; (D) 2.0 μM dC_{12}–Ag NCs, 8 μM ATCh chloride and 0.002 U/mL AChE. 5.0 mM sodium phosphate buffer, pH 7.0.

Fluorescence Turn-on AChE Assay. The application of dC_{12}–Ag NCs and ATCh chloride for AChE activity assay was demonstrated. The AChE activity was determined using the Ellman method for validation (Supporting Information S5) and successively diluted for further use. First, the solution of dC_{12}–Ag NCs (2.0 μM) and ATCh chloride (8.0 μM) exhibited a weak fluorescence. After the addition of AChE (0.001 U/mL), the fluorescence intensity gradually increased by prolonging the incubation time (Figure 4). For instance, the fluorescence

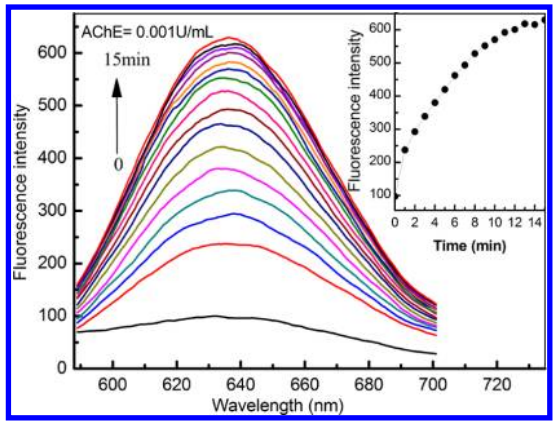

Figure 4. Fluorescence spectra of the ensemble of 2.0 μM dC_{12}–Ag NCs and ATCh chloride (8.0 μM) in the presence of AChE (0.001 U/mL) incubated at room temperature for different periods. The inset is the plot of fluorescence intensity of dC_{12}–Ag NCs at 635 nm versus the incubation time.

intensity at 635 nm was enhanced by ~6.5 times after AChE (0.001 U/mL) was introduced, and the solution was incubated at room temperature for 15 min. The control experiments confirmed that the fluorescence enhancement observed for dC_{12}–Ag NCs requires the presence of both ATCh chloride and AChE. Neither the ensemble of dC_{12}–Ag NCs/AChE nor that of dC_{12}–Ag NCs/ATCh chloride exhibited fluorescence enhancement (Figure 3). Therefore, the increase of the fluorescence of the ensemble of dC_{12}–Ag NCs and ATCh chloride after the addition of AChE can be understood as follows: ATCh chloride was hydrolyzed to generate TCh, which reacted with dC_{12}–Ag NCs to form a complex, thereby

dx.doi.org/10.1021/ac401966d | Anal. Chem. 2013, 85, 8455−8461

enhancing the fluorescence. It should be noted that the other commonly used substrate for AChE, ATCh iodide, cannot be used as an alternative to ATCh chloride as substrate in this experiment because of the quenching effect of iodide ion on the fluorescence of dC_{12}–Ag NCs (Figure S4, Supporting Information).

The fluorescence spectra of dC_{12}–Ag NCs (2.0 μM) and ATCh (8.0 μM) chloride containing different concentrations of AChE were measured after incubation for different periods, respectively, to determine the sensitivity of the protocol. The fluorescence intensity of DNA-Ag NCs at 635 nm was then plotted as a function of AChE incubation time (up to 5 min). The change in fluorescence intensity per unit time, which represents the activity of AChE, was calculated from the slope of each straight line. As shown in Figure 5, the fluorescence

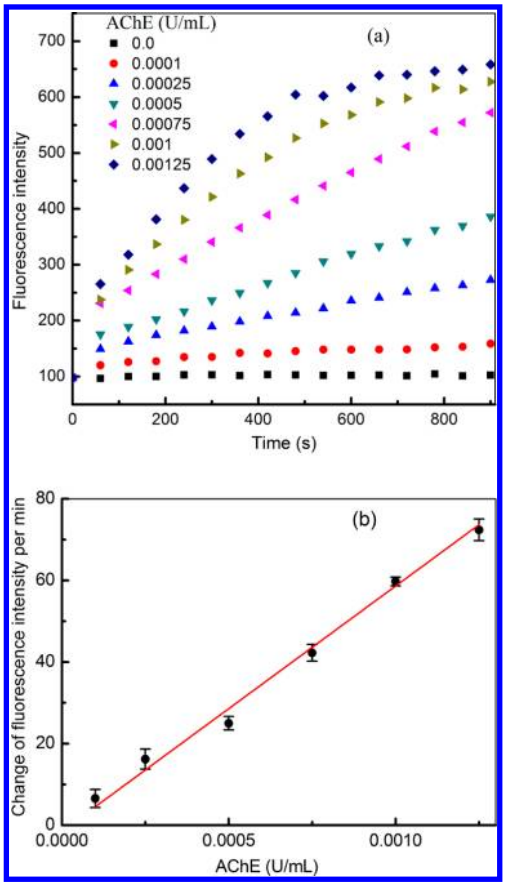

Figure 5. (a). Variation of the fluorescence intensity at 635 nm versus the reaction time for the dC_{12}–Ag NCs (2.0 μM) and ATCh chloride (8.0 μM) in the presence of different concentrations of AChE. The excitation wavelength was 570 nm. (b) The changes of fluorescence intensity per min at 635 nm as a function of the activity of AChE.

intensity at 635 nm remained almost constant in the absence of AChE; however, the fluorescence intensity gradually increased in the presence of AChE by prolonging the reaction time at room temperature.

Evidently, a large degree of fluorescence enhancement was detected, containing high concentrations of AChE. This observation is attributed to the increased formation of TChs by more AChEs, which conjugate to dC_{12}–Ag NCs leading to fluorescence enhancement. Due to the sensitive and rapid fluorescence turn-on response of dC_{12}–Ag NCs to TCh, AChE with concentrations as low as 0.5×10^{-4} U/mL (signal/noise = 3) can be analyzed with a dynamic range of 0.1×10^{-3} U/mL to 1.25×10^{-3} U/mL (R^2 = 0.9898). This "mix-and-detect" method is not involved in complicated cascade reactions and uses commercial ATCh chloride as substrate, and dC_{12}–Ag NCs can be prepared without laborious procedures.

As with Ellmans's reagent, dC_{12}–Ag NCs elicited the same effect on other thiol compounds, such as reduced GSH and Cys. However, the degree of fluorescence enhancement of dC_{12}–Ag NCs in the presence of GSH/Cys was lower than that of dC_{12}–Ag NCs alone after incubation with TCh under the same conditions (Figure S5, Supporting Information). Moreover, given that TCh is produced by the AChE hydrolysis of ATCh chloride, the interference of thiol-containing compounds, such as GSH and Cys, can be eliminated through the following ways.[27] First, the sample under investigation was mixed with dC_{12}–Ag NCs, the solution was incubated, and then the fluorescence intensity was measured. Second, the same amount of sample was mixed with dC_{12}–Ag NCs, ATCh chloride, and AChE, the solution was incubated, and then the fluorescence intensity was measured. Third, the difference in fluorescence intensity between the above two cases was used for the AChE activity assay.

To evaluate the specificity of the fluorometric assay to AChE, many proteins or enzymes, including CIAP, lipase, Lys, and HSA, were tested (Figure 6). The fluorescence of dC_{12}–Ag

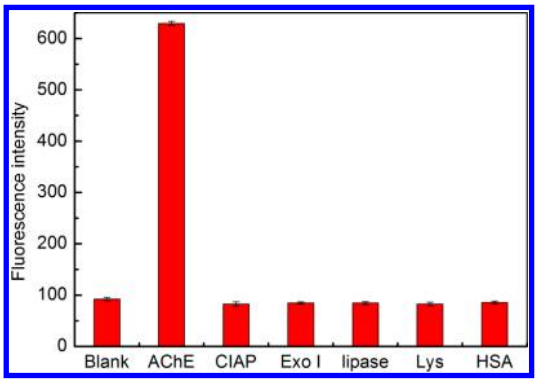

Figure 6. Fluorescence intensity at 635 nm for the dC_{12}–AgNCs (2.0 μM) in the presence of ATCh chloride (8.0 μM) incubation with AChE (0.001U/mL), CIAP (0.1U/mL), Exo I (0.1U/mL), lipase (0.1U/mL), Lys (0.1U/mL), and HSA (0.04 mg/mL) and blank for 15 min.

NCs at 635 nm increased distinctly with the addition of AChE but only slightly changed with the addition of CIAP, Exo I, lipase, Lys, and HSA. These results indicate that the fluorometric dC_{12}–Ag NC-based assay exhibits high selectivity to AChE.

AChE Inhibition Assay. The dC_{12}–Ag NCs described in the present study can be used to screen AChE inhibitors because the hydrolysis of ATCh chloride catalyzed by AChE becomes retarded in the presence of corresponding AChE inhibitors. Tacrine, a typical inhibitor of AChE, was selected to demonstrate the application. The fluorescence intensity of dC_{12}–Ag NCs (2.0 μM), which contained 0.75×10^{-3} U/mL AChE and incubated with different concentrations of tacrine for 15 min at room temperature, were recorded at 635 nm as a function of time, respectively (Figure 7a). The inhibition efficiency was determined by formula, $[A_0 - A_i/A_0] \times 100$, as described in detail in the Experimental Section. Based on the plot of the inhibition efficiency versus the concentration of

dx.doi.org/10.1021/ac401966d | Anal. Chem. 2013, 85, 8455–8461

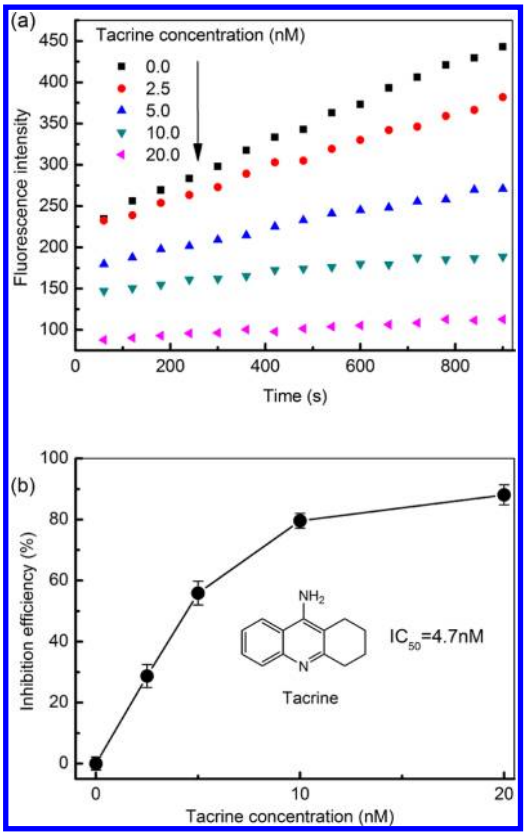

Figure 7. (a) Plot of the fluorescence intensity at 635 nm versus the incubation time for the ensemble of the 2.0 μM dC_{12}–Ag NCs and ATCh chloride (8.0 μM) containing AChE (0.00075 U/mL) in the presence of different concentrations of tacrine; (b) Plot of the inhibition efficiency for AChE versus the concentration of tacrine.

tacrine (Figure 7b), the corresponding IC_{50} value was 4.7 ± 0.7 nM. It was different from the IC_{50} values reported before.[7b,28] However, it is understandable, since the IC_{50} values usually increase by increasing the enzyme concentration.[7b] Similarly, the IC_{50} value of galanthamine was determined to be 14.8 ± 0.5 nM (Supporting Information, Figure S6). The proposed method permitted the use of lower enzyme amounts and lower substrate concentrations, which was more cost-efficient and favorable than existing methods for screening inhibitors with IC_{50} values at or below the nM scale.

Detecting AChE Activity in Human RBC Membranes. Measurement results of AChE activity with dC_{12}–Ag NCs in human RBC membranes were validated against Ellman's method. Five fresh blood samples from healthy individuals were provided by the Third Affiliated Hospital, Xi'an Jiaotong University, according to the rules of the local ethical committee. Human RBC membranes were prepared as described in the Experimental Section and used for dC_{12}–Ag NC measurements. A fraction of each sample was analyzed by Ellman's method. All obtained results from dC_{12}–Ag NCs measurements showed acceptable agreement with the data using the standard Ellman's method (Table 1). Student's t test at $P = 0.9$ revealed no statistically significant difference between the results obtained using the dC_{12}–Ag NC method developed in this work and those obtained using Ellman's method. This result indicates that the proposed dC_{12}–Ag NC method is reliable for AChE activity assay.

CONCLUSION

The present study introduced a highly sensitive fluorometric method for AChE activity assay. This assay is designed using the following features: (1) catalytic hydrolysis of ATCh chloride to TCh by AChE and (2) the fluorescence turn-on of dC_{12}–Ag NCs via its reactions with TCh. The assay can be distinguished from other biothiol compounds in biological samples because of the TCh content from enzymatic hydrolysis. The enhanced fluorescence pattern also inherited the high specificity in compassion to fluorescence quenching pattern because other quenchers or environmental stimuli can also lead to fluorescence reduction. The assay offers the benefits of extremely low background noise and high detection sensitivity. A detection limit of 0.5×10^{-4} U/mL AChE was obtained. Furthermore, the simple "mix-and-detect" detection format and rapid chemical reactions were comparable to the widely used Ellman method and can be expanded to a range of important areas, such as neurobiology, toxicology, and pharmacology for AChE activity assay.

ASSOCIATED CONTENT

Supporting Information

Ellman method for validation, Table S1, and Figures S1–S6. This material is available free of charge via the Internet at http://pubs.acs.org.

AUTHOR INFORMATION

Corresponding Author

*Phone: +86-29-81530726. Fax: +86-29-81530727. E-mail: ydzhang@snnu.edu.cn.

Notes

The authors declare no competing financial interest.

ACKNOWLEDGMENTS

We would like to thank Prof. Dr. C. Zhang and Q. Gao for their kind assistance. This work was supported by the National Natural Science Foundation of China (21275097, 30600494), the Fundamental Research Fund for the Central Universities (GK201303001), and the Program for Changjiang Scholars and Innovative Research Team in University (IRT 1070).

Table 1. Measurement of AChE Activity in Human RBC Membranes[a]

RBC samples no.	1 (man)	2 (woman)	3 (woman)	4 (man)	5 (man)
RBC counting ($\times 10^{12}$/L)[b]	4.61	4.36	4.64	4.16	4.94
Ellman method (nU/RBC)[c]	1.26 ± 0.11	1.30 ± 0.13	1.19 ± 0.16	1.28 ± 0.12	1.18 ± 0.18
this method (nU/RBC)[c]	1.24 ± 0.17	1.36 ± 0.19	1.23 ± 0.13	1.32 ± 0.17	1.24 ± 0.14

[a]AChE activity was calculated by the obtained signal response (the change in fluorescence intensity per min) and the calibration curve. For both AChE activities, the values were calculated per RBC. [b]An automatic hemocytometer was used for RBC counting. [c]Confidence interval ($n = 3$, $P = 0.9$).

REFERENCES

(1) (a) Xuereb, J. H.; Perry, E. K.; Candy, J. M.; Bonham, J. R.; Perry, R. H.; Marshall, E. J. *Neurol. Sci.* **1990**, *99*, 185−197. (b) Coggan, J. S.; Bartol, T. M.; Esquenazi, E.; Stiles, J. R.; Lamont, S.; Martone, M. E.; Berg, D. K.; Ellisman, M. H.; Sejnowski, T. J. *Science* **2005**, *309*, 446−451.

(2) Dvir, H.; Silman, I.; Harel, M.; Rosenberry, T. L.; Sussman, J. L. *Chem. Biol. Interact.* **2010**, *187*, 10−22.

(3) Musial, A.; Bajda, M.; Malawska, B. *Curr. Med. Chem.* **2007**, *14*, 2654−2679.

(4) (a) Ellman, G. L.; Courtney, K. D.; Andres, V.; Featherstone, R. M. *Biochem. Pharmacol.* **1961**, *7*, 88−95. (b) Holas, O.; Musilek, K.; Pohanka, M.; Kuca, K. *Expert. Opin. Drug Discovery* **2012**, *7*, 1207−1223.

(5) Riddles, P. W.; Blakeley, R. L.; Zerner, B. *Anal. Biochem.* **1979**, *94*, 75−81.

(6) Worek, F.; Mast, U.; Kiderlen, D.; Diepold, C.; Eyer, P. *Clin. Chim. Acta* **1999**, *288*, 73−90.

(7) (a) Miao, Y.; He, N.; Zhu, J. J. *Chem. Rev.* **2010**, *110*, 5216−5234. (b) Wang, M.; Gu, X.; Zhang, G.; Zhang, D.; Zhu, D. *Langmuir* **2009**, *25*, 2504−2507. (c) Sabelle, S.; Renard, P. Y.; Pecorella, K.; Suzzoni-Dezard, S. De; Creminon, C.; Grassi, J.; Mioskowski, C. *J. Am. Chem. Soc.* **2002**, *124*, 4874−4880. (d) Peng, L.; Zhang, G.; Zhang, D.; Xiang, J.; Zhao, R.; Wang, Y.; Zhu, D. *Org. Lett.* **2009**, *11*, 4014−4017. (e) Wang, M.; Gu, X.; Zhang, G.; Zhang, D.; Zhu, D. *Anal. Chem.* **2009**, *81*, 4444−4449. (f) Feng, F.; Tang, Y.; Wang, S.; Li, Y.; Zhu, D. *Angew. Chem., Int. Ed.* **2007**, *46*, 7882−7886. (g) Saa, L.; Virel, A.; Sanchez-Lopez, J.; Pavlov, V. *Chem.—Eur. J.* **2010**, *16*, 6187−6192. (h) Zhang, W.; Zhu, L.; Qin, J.; Yang, C. *J. Phys. Chem. B* **2011**, *115*, 12059−12064. (i) Shen, X.; Liang, F.; Zhang, G.; Zhang, D. *Analyst* **2012**, *137*, 2119−2123. (j) Zhao, W.; Sun, S. X.; Xu, J. J.; Chen, H. Y.; Cao, X. J.; Guan, X. H. *Anal. Chem.* **2008**, *80*, 3769−3776. (k) Haddad, G. L.; Young, S. C.; Heindel, N. D.; Bornhop, D. J.; Flowers, R. A. *Angew. Chem., Int. Ed.* **2012**, *51*, 11126−11130. (l) Liao, D.; Chen, J.; Zhou, H.; Wang, Y.; Li, Y.; Yu, C. *Anal. Chem.* **2013**, *85*, 2667−2672.

(8) Das, S.; Powe, A. M.; Baker, G. A.; Valle, B.; El-Zahab, B.; Sintim, H. O.; Lowry, M.; Fakayode, S. O.; McCarroll, M. E.; Patonay, G.; Li, M.; Strongin, R. M.; Geng, M. L.; Warner, I. M. *Anal. Chem.* **2012**, *84*, 597−625.

(9) (a) Algar, W. R.; Susumu, K.; Delehanty, J. B.; Medintz, I. L. *Anal. Chem.* **2011**, *83*, 8826−8837. (b) Ozawa, T.; Yoshimura, H.; Kim, S. B. *Anal. Chem.* **2013**, *85*, 590−609.

(10) (a) Petty, J. T.; Zheng, J.; Hud, N. V.; Dickson, R. M. *J. Am. Chem. Soc.* **2004**, *126*, 5207−5212. (b) Guo, W.; Yuan, J.; Dong, Q.; Wang, E. *J. Am. Chem. Soc.* **2010**, *132*, 932−934. (c) Pal, S.; Varghese, R.; Deng, Z.; Zhao, Z.; Kumar, A.; Yan, H.; Liu, Y. *Angew. Chem., Int. Ed. Engl.* **2011**, *50*, 4176−4179. (d) Yeh, H. C.; Sharma, J.; Shih, I.; Vu, D. M.; Martinez, J. S.; Werner, J. H. *J. Am. Chem. Soc.* **2012**, *134*, 11550−11558. (e) Li, J.; Zhong, X.; Zhang, H.; Le, X. C.; Zhu, J. J. *Anal. Chem.* **2012**, *84*, 5170−5174. (f) Han, B.; Wang, E. *Anal. Bioanal. Chem.* **2012**, *402*, 129−138. (g) Antoku, Y.; Hotta, J.; Mizuno, H.; Dickson, R. M.; Hofkens, J.; Vosch, T. *Photochem. Photobiol. Sci.* **2010**, *9*, 716−721. (h) Ritchie, C. M.; Johnsen, K. R.; Kiser, J. R.; Antoku, Y.; Dickson, R. M.; Petty, J. T. *J. Phys. Chem. C* **2007**, *111*, 175−181. (i) Yeh, H. C.; Sharma, J.; Han, J. J.; Martinez, J. S.; Werner, J. H. *Nano Lett.* **2010**, *10*, 3106−3110. (j) Choi, S.; Yu, J.; Patel, S. A.; Tzeng, Y. L.; Dickson, R. M. *Photochem. Photobiol. Sci.* **2011**, *10*, 109−115.

(11) Yu, J.; Choi, S.; Richards, C. I.; Antoku, Y.; Dickson, R. M. *Photochem. Photobiol.* **2008**, *84*, 1435−1439.

(12) Sharma, J.; Yeh, H. C.; Yoo, H.; Werner, J. H.; Martinez, J. S. *Chem. Commun. (Cambridge, U. K.)* **2011**, *47*, 2294−2296.

(13) Han, B.; Wang, E. *Biosens. Bioelectron.* **2011**, *26*, 2585−2589.

(14) Huang, Z.; Pu, F.; Lin, Y.; Ren, J.; Qu, X. *Chem. Commun. (Cambridge, U. K.)* **2011**, *47*, 3487−3489.

(15) Hammond, P. I.; Kern, C.; Hong, F.; Kollmeyer, T. M.; Pang, Y. P.; Brimijoin, S. *J. Pharmacol. Exp. Ther.* **2003**, *307*, 190−196.

(16) Harbich, W.; Fedrigo, S.; Meyer, F.; Lindsay, D. M.; Lignieres, J.; Rivoal, J. C.; Kreisle, D. *J. Chem. Phys.* **1990**, *93*, 8535−8543.

(17) Bonacic-Koutecký, V.; Pittner, J.; Boiron, M.; Fantucci, P. *J. Chem. Phys.* **1999**, *110*, 3876−3886.

(18) Daune, M.; Dekker, C. A.; Schachman, H. K. *Biopolymers* **1966**, *4*, 51−76.

(19) (a) Huang, C. C.; Yang, Z.; Lee, K. H.; Chang, H. T. *Angew. Chem., Int. Ed. Engl.* **2007**, *46*, 6824−6828. (b) Wu, Z.; Jin, R. *Nano Lett.* **2010**, *10*, 2568−2573.

(20) Bachman, R. E.; Bodolosky-Bettis, S. A.; Glennon, S. C.; Sirchio, S. A. *J. Am. Chem. Soc.* **2000**, *122*, 7146−7147.

(21) Yam, V. W.-W.; Lo, K. K.-W. *Chem. Soc. Rev.* **1999**, *28*, 323−334.

(22) Taleb, A.; Petit, C.; Pileni, M. P. *Chem. Mater.* **1997**, *9*, 950−959.

(23) Kaushik, V. K. J. *Electron Spectrosc. Relat. Phenom.* **1991**, *56*, 273−277.

(24) (a) Santos, E.; Avalle, L.; Pötting, K.; Vélez, P.; Jones, H. *Electrochim. Acta* **2008**, *53*, 6807−6817. (b) Luque, N. B.; Vélez, P.; Pötting, K.; Santos, E. *Langmuir* **2012**, *28*, 8084−8099.

(25) Luque, N. B.; Santos, E. *Langmuir* **2012**, *28*, 11472−11480.

(26) Harel, M.; Schalk, I.; Ehret-Sabatier, L.; Bouet, F.; Goeldner, M.; Hirth, C.; Axelsen, P. H.; Silman, I.; Sussman, J. L. *Proc. Natl. Acad. Sci. U. S. A* **1993**, *90*, 9031−9035.

(27) Cui, K.; Chen, Z.; Wang, Z.; Zhang, G.; Zhang, D. *Analyst* **2011**, *136*, 191−195.

(28) Liston, D. R.; Nielsen, J. A.; Villalobos, A.; Chapin, D.; Jones, S. B.; Hubbard, S. T.; Shalaby, I. A.; Ramirez, A.; Nason, D.; White, W. F. *Eur. J. Pharmacol.* **2004**, *486*, 9−17.